Comprehensive *In Vitro* Characterization of *CXCR4*^{WHIM} Variants to Decipher Genotype–Phenotype Correlations in WHIM Syndrome

Katarina Zmajkovicova,[1] Sabine Maier-Munsa,[1] Barbara Maierhofer,[1] Arthur G. Taveras,[2] Adriana Badarau[3]

[1]X4 Pharmaceuticals (Austria) GmbH, Vienna, Austria; [2]X4 Pharmaceuticals, Inc., Boston, MA, USA; [3]Formerly of X4 Pharmaceuticals

Poster # 2063

Background

- WHIM (Warts, Hypogammaglobulinemia, Infections, Myelokathexis) syndrome is a rare, autosomal-dominant primary immunodeficiency with neutropenia and lymphopenia[1-3]
- The clinical presentation of WHIM syndrome may include recurrent infections and increased susceptibility to human papillomavirus[2]
- In >80% of cases, WHIM syndrome is caused by heterozygous gain-of-function (GOF) mutations in C-X-C chemokine receptor 4 (CXCR4), with 16 known pathogenic variants reported in WHIM syndrome to date (nonsense [NS], frameshift [FS], and missense [MS]) spanning 27 C-terminal amino acids (Figure 1A)[2-7]
- These mutations cause hyperactivation of downstream signaling and retention of white blood cells (WBCs) in the bone marrow (Figure 1B)[3]

Figure 1: *CXCR4* Variants and Functional Consequences of CXCR4 Receptor Mutations in WHIM Syndrome

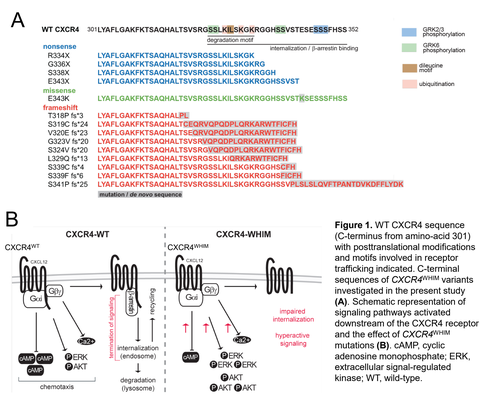

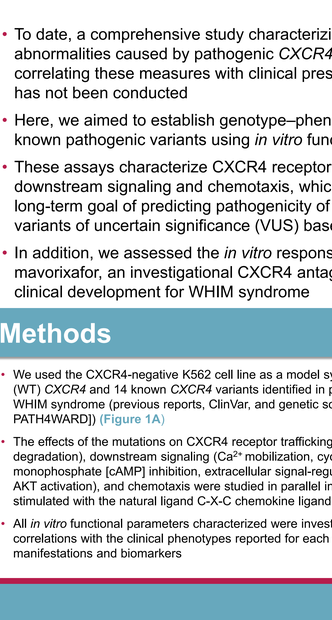

Figure 1. WT CXCR4 sequence (C-terminus from amino-acid 301) with posttranslational modifications and motifs involved in receptor trafficking indicated. C-terminal sequences of *CXCR4*^{WHIM} variants investigated in the present study **(A)**. Schematic representation of signaling pathways activated downstream of the CXCR4 receptor and the effect of *CXCR4*^{WHIM} mutations **(B)**. cAMP, cyclic adenosine monophosphate; ERK, extracellular signal-regulated kinase; WT, wild-type.

- To date, a comprehensive study characterizing the functional abnormalities caused by pathogenic *CXCR4* mutations and correlating these measures with clinical presentation in patients has not been conducted
- Here, we aimed to establish genotype–phenotype correlations for known pathogenic variants using *in vitro* functional assays
- These assays characterize CXCR4 receptor trafficking, downstream signaling and chemotaxis, which will enable the long-term goal of predicting pathogenicity of novel *CXCR4* variants of uncertain significance (VUS) based on *in vitro* assays
- In addition, we assessed the *in vitro* response of each variant to mavorixafor, an investigational CXCR4 antagonist currently in clinical development for WHIM syndrome

Methods

- We used the CXCR4-negative K562 cell line as a model system to express wild-type (WT) *CXCR4* and 14 known *CXCR4* variants identified in patients diagnosed with WHIM syndrome (previous reports, ClinVar, and genetic screening initiatives [Invitae PATH4WARD]) (Figure 1A)
- The effects of the mutations on CXCR4 receptor trafficking (internalization and degradation), downstream signaling (Ca^{2+} mobilization, cyclic adenosine monophosphate [cAMP] inhibition, extracellular signal-regulated kinase [ERK] and AKT activation), and chemotaxis were studied in parallel in a series of assays in cells stimulated with the natural ligand C-X-C chemokine ligand 12 (CXCL12)
- All *in vitro* functional parameters characterized were investigated for potential correlations with the clinical phenotypes reported for each variant, including disease manifestations and biomarkers

Results

CXCR4^{WHIM} variants exhibited impaired receptor internalization in response to CXCL12

- Impaired receptor internalization in response to CXCL12 was observed, evidenced by higher percentage of CXCR4^{WHIM} receptors remaining on the cell surface compared to WT CXCR4, with NS and FS variants showing maximum impairment and the MS variant E343K being least affected at the two time points studied (Figure 2)

Figure 2: *CXCR4* Variants and Receptor Internalization

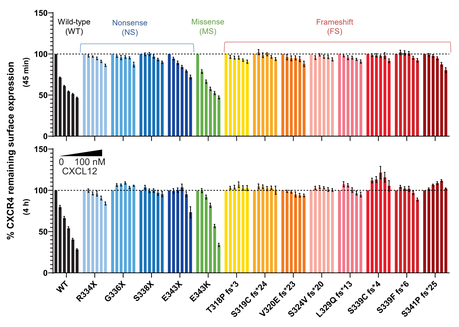

Figure 2. Serum-starved K562 cells with stable CXCR4 expression were stimulated with CXCL12 (vehicle, 1.2 nM, 3.7 nM, 11 nM, 33 nM, 100 nM) for 45 minutes or 4 hours, and the surface expression of CXCR4 was measured by flow cytometry. Values are expressed as % remaining CXCR4 compared to vehicle-treated cells. Values represent mean +/- SEM of 4 clonal lines per variant analyzed in 4 independent experiments.

CXCR4^{WHIM} variants exhibited decreased CXCR4 degradation and increased cAMP inhibition

- The decreased CXCR4 internalization correlated with decreased CXCR4 protein degradation and increased cAMP inhibition (Figure 3)

Figure 3: Correlation of CXCR4 Internalization With Receptor Degradation and cAMP Inhibition

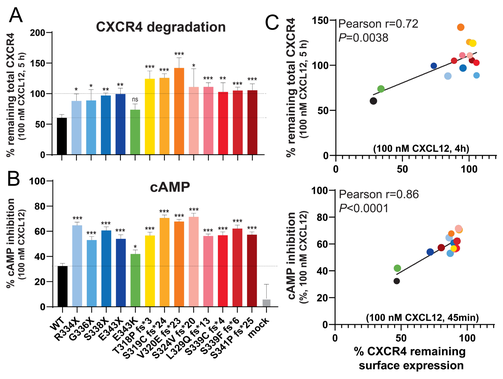

Figure 3. Serum-starved K562 cells with stable CXCR4 expression were stimulated with vehicle or 100 nM CXCL12 for 5 hours, and the whole-cell lysates were analyzed by western blot to determine total CXCR4 levels. Samples from individual clonal lines were pooled per variant in each experiment. Values represent % of treated sample compared to vehicle control. Mean +/- SEM, n=3–4 **(A)**. Serum-starved K562 cells with stable CXCR4 expression were stimulated with forskolin +/- 100 nM CXCL12 for 30 minutes. cAMP production was measured by ELISA. % inhibition of cAMP production by CXCL12 was calculated respective to forskolin-only treated cells. Values represent mean +/- SEM of 4 clonal lines per variant analyzed in 4 independent experiments **(B)**. Plots showing correlation between CXCR4 degradation/CXCR4 internalization (upper panel) and cAMP inhibition/CXCR4 internalization (lower panel). Linear regression was used to analyze the correlation of measured values **(C)**. ELISA, enzyme-linked immunosorbent assay.

CXCR4^{WHIM} variants demonstrated a higher amplitude and duration of AKT and ERK activation in response to CXCL12 stimulation (Figure 4)

Figure 4: *CXCR4* Variants and AKT and ERK Activation

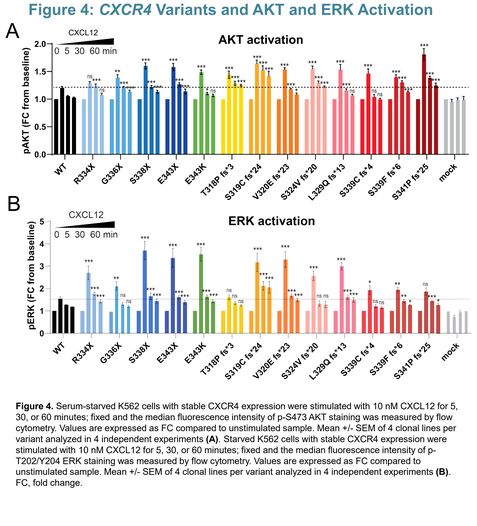

Figure 4. Serum-starved K562 cells with stable CXCR4 expression were stimulated with 10 nM CXCL12 for 5, 30, or 60 minutes; fixed and the median fluorescence intensity of p-S473 AKT staining was measured by flow cytometry. Values are expressed as FC compared to unstimulated sample. Mean +/- SEM of 4 clonal lines per variant analyzed in 4 independent experiments **(A)**. Starved K562 cells with stable CXCR4 expression were stimulated with 10 nM CXCL12 for 5, 30, or 60 minutes; fixed and the median fluorescence intensity of p-T202/Y204 ERK staining was measured by flow cytometry. Values are expressed as FC compared to unstimulated sample. Mean +/- SEM of 4 clonal lines per variant analyzed in 4 independent experiments **(B)**. FC, fold change.

CXCR4^{WHIM} variants showed increased chemotaxis toward CXCL12

- Chemotactic responses to CXCL12 were diverse, depending on the variant sequence and subtype. For the more truncated FS variants (T318Pfs*3, S319Cfs*24, V320Efs*23), chemotaxis increased only at higher CXCL12 concentrations; other FS variants showed enhanced chemotaxis regardless of CXCL12 concentration (Figure 5)

Figure 5: *CXCR4* Variants and Chemotaxis

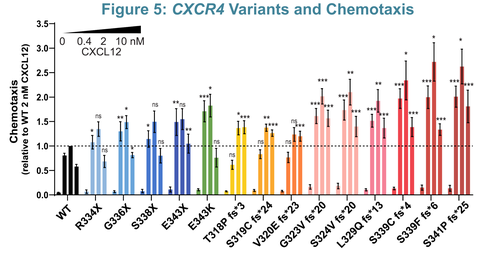

Figure 5. Serum-starved K562 cells transiently transfected with indicated CXCR4 constructs were subjected to trans-well chemotaxis assay. Cells migrated toward 0.4, 2, 10 nM CXCL12 or medium only for 4 hours. The total number of migrated cells was normalized to WT with 2 nM CXCL12 in each assay. Mean +/- SEM, n=4–14.

Mavorixafor inhibited Ca^{2+} mobilization and CXCL12-dependent downstream signaling in all *CXCR4* mutant cells

- Mavorixafor inhibited Ca^{2+} mobilization in *CXCR4*^{WT} and all *CXCR4*^{WHIM} variants (half maximal inhibitory concentration [IC_{50}]=7.6–39 nM; maximum effect [E_{max}]=51%–90%) (Figure 6A)
- Mavorixafor also prevented CXCL12-induced hyperactivation of ERK and AKT in all *CXCR4*^{WHIM} variants (Figure 6B)

Figure 6: Mavorixafor Treatment Effects on Ca^{2+} Mobilization, ERK and AKT Signaling

A

Ca^{2+} mobilization	WT	R334X	G336X	S338X	E343X	E343K	T318P fs*3	S319C fs*24	V320E fs*23	S324V fs*20	L329Q fs*13	S339C fs*4	S339F fs*6	S341P fs*25
mavorixafor IC50 (nM)	6.3	15	11.8	7.7	8.8	19.4	7.6	39	17	37.9	19.3	8.6	26.7	18.2
mavorixafor Emax (%)	84	72	82	89	90	66	88	76	65	58	51	77	59	57

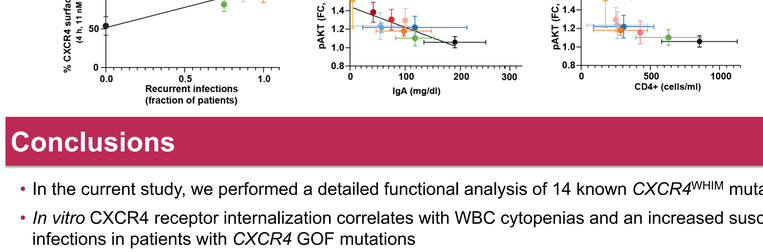

Figure 6. E_{max} (% inhibition) and IC_{50} values of mavorixafor determined in Ca^{2+} mobilization assays. Starved K562 cells with stable CXCR4 expression were preincubated with serial dilutions of mavorixafor and then stimulated with 10 nM CXCL12. Mean +/- SEM, n=4–17 **(A)**. Profiling of mavorixafor in ERK activation assays. Serum-starved K562 cells with stable CXCR4 expression were preincubated with 40 nM, 200 nM, or 1 µM mavorixafor and then stimulated with 10 nM CXCL12 for 5 minutes. Median fluorescence intensity of p-T202/Y204 ERK staining was measured by flow cytometry. Values are expressed as % maximal induction in the vehicle-treated cells. Mean +/- SEM, n=3–17 **(B)**. Profiling of mavorixafor in AKT activation assay. Serum-starved K562 cells with stable CXCR4 expression were preincubated with 40 nM, 200 nM or 1 µM mavorixafor and then stimulated with 10 nM CXCL12 for 5 minutes. The median fluorescence intensity of p-S473 AKT staining was measured by flow cytometry. Values are expressed as % maximal induction in the vehicle-treated cells. Mean +/- SEM, n=3–14 **(C)**.

In vitro functional parameters correlated with the clinical phenotypes reported for patients with WHIM syndrome (Figure 7)

Figure 7: *CXCR4*^{WHIM} Variants and Correlation of Function With Clinical Phenotype

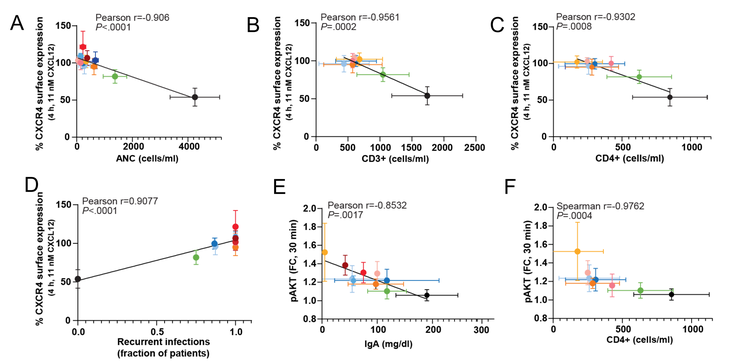

Figure 7. Correlation between ANC and CXCR4 internalization **(A)**, CD3+ cells and CXCR4 internalization **(B)**, CD4+ cells and CXCR4 internalization **(C)**, recurrent infection rates and CXCR4 internalization **(D)**, pAKT and IgA levels **(E)**, and pAKT and CD4+ cells **(F)**. Linear regression was used to analyze the correlation of measured values in **A-E**; Spearman correlation was used in **F**. Values are plotted as mean (SD). CD, cluster of differentiation; IgA, immunoglobulin A, pAKT, phosphorylated AKT.

- The CXCR4 internalization defect demonstrated for each *CXCR4*^{WHIM} variant strongly correlated with the absolute neutrophil count (ANC) and absolute CD3$^+$ and CD4$^+$ T-cell count in peripheral blood of patients carrying the respective *CXCR4*^{WHIM} mutation
- There was a direct correlation of the impairment of CXCR4 receptor internalization with susceptibility to recurrent infections in patients with WHIM syndrome
- Other correlations include AKT hyperactivation, associated with lower IgA levels and decreased CD4$^+$ T-cell counts

Conclusions

- In the current study, we performed a detailed functional analysis of 14 known *CXCR4*^{WHIM} mutations
- *In vitro* CXCR4 receptor internalization correlates with WBC cytopenias and an increased susceptibility to recurrent infections in patients with *CXCR4* GOF mutations
- These data suggest that CXCR4 internalization and AKT activation may be used as key assays for the prediction of known *CXCR4* variant pathogenicity *in vitro* and potentially as WHIM-related disease biomarkers
- Additionally, all tested *CXCR4* variant cell lines were sensitive to mavorixafor at clinically relevant concentrations, rescuing defective GOF signaling. Mavorixafor also inhibited CXCL12-induced signaling downstream of WT CXCR4

Acknowledgements

The authors would like to thank everyone involved in the clinical development of mavorixafor and acknowledge the medical writing assistance of PRECISIONscientia in Yardley, PA, USA, which was supported financially by X4 Pharmaceuticals in compliance with international Good Publication Practice guidelines.

Disclosures

KZ, SM, BM, and **AGT** are current employees of X4 Pharmaceuticals and/or have equity ownership. **AB** is a former employee of X4 Pharmaceuticals and has equity ownership.

References

1. Wetzler M, et al. *Am J Med.* 1990;89:663-672. **2.** McDermott DH, Murphy PM. *Immunol Rev.* 2019;287:91-102. **3.** Beaussant Cohen S, et al. *Orphanet J Rare Dis.* 2012;7:71. **4.** Dotta L, et al. WHIM syndrome: clinical phenotype and therapeutic measures of a cohort of 21 patients. Poster presented at: ESID; September 21–24, 2016; Barcelona, Spain. **5.** Shin DW, et al. *Ann Lab Med.* 2017;37:446-449. **6.** Badolato R, et al. *Blood.* 2017;130(23):2491-2498. **7.** Dale D, et al. *Blood.* 2020;136(26):2994-3003.